Theoretical Study of Elementary Steps in the Reactions between Aluminum and Teflon Fragments under Combustive Environments

Martin Losada and Santanu Chaudhuri*

Applied Sciences Laboratory, Washington State University, Spokane, Washington 99210-1495

Received: November 18, 2008; Revised Manuscript Received: February 4, 2009

Gas-phase reactions between aluminum particles and Teflon fragments were studied to develop a fundamental understanding of the decomposition reactions and combustion processes of the Al−Teflon composites. The reactions were investigated theoretically using ab initio calculations at the MP2/aug-cc-pVDZ level, with the final thermokinetic data obtained with coupled cluster theory (CCSD(T)/aug-cc-pVTZ). Among reactions under oxygen-lean conditions, $CF_3 + Al \rightarrow CF_2 + AlF$ channel is the fastest, followed by the $CF_2 + Al \rightarrow CF + AlF$ and $CF + Al \rightarrow C + AlF$ channels. Under oxygen-rich conditions, reactions of COF with aluminum are probed to be faster than those involving COF_2 species. Reaction path multiplicity has been considered. Our results show that multiplicity plays a very important role in determining the reaction order, that is first order or addition−elimination reactions of Al with CF_3 are predicted to be faster than those proceeding through direct abstraction or second order. In addition, the present kinetic model suggests that $CF_3 + Al \rightarrow CF_2 + AlF$ with $m = 1$ and $COF + Al \rightarrow CO + AlF$ channels are very competitive under the same thermal conditions. The computed enthalpies of reaction are systematically compared with the available literature. The predicted kinetic model and its time constants (τ) are in good qualitative agreement with experimental observations of the reactions between Al nanoparticles and Teflon for the 500−1200 K temperature range.

1. Introduction

Energetic materials include propellants, explosives, and pyrotechnics. These materials can be thought of as controllable storage systems for chemical energy. Energetic materials have numerous military and industrial applications. There is a continuing need for improved energetic materials. In developing new energetic materials, one seeks optimal trade-offs in energy content, energy release, safety, and cost. There are significant costs associated with development of a new material. Therefore, it is important to reduce the amount of trial and error in new material development by predicting energetic material properties and behavior. The energy content of an energetic material often determines its practical utility. The useful energy content is determined by the anticipated release mechanism. Thus, the thermodynamics and the time scale of the chemical reactions involved are crucial to understand the chemistry behind these materials and the associated fundamental mechanism. It is still largely unknown which bond in the molecule of a certain energetic material breaks first and what type of chemical reactions (unimolecular versus bimolecular, etc.) occur first. However, applications of ultrafast spectroscopic methods hold great promise for understanding these basic mechanisms at the molecular level through spectroscopic measurements. Review of previous work in this field can be found in the literature.[1]

Energetic materials exist in a higher energy state than their lowest-energy decomposition products. Thus, energetic molecules are often termed metastable. Kinetic stability, however, guarantees that decomposition is sufficiently slow at ambient conditions so that the species are long-lived. A new class of thermites referred to as metastable intermolecular composites (MIC) has been described as "mixtures of nanoscale powders of reactants that exhibit thermite (high exothermicity) behavior".[2] This new class of composites utilizes nanoscale powders that result in much higher propagation rates and ignition sensitivity than their micro-scale counterparts.[3,4] One particularly interesting MIC is that composed of Al nanoparticles embedded in a Teflon oxidizer, Al−Teflon. This is one of the most exothermic compositions suitable for nanoenergetic materials with a theoretical heat of combustion of 21 kJ/cm^3,[5,6] compared for instance to only 8 kJ/cm^3 for TNT.[7]

Numerous studies of the decomposition reactions and combustion processes of the Al/Teflon composites have been published. Parker et al.[8] investigated the Al−Teflon combustion by high-pressure time-resolved absorption spectroscopy. In that work, the authors suggested that the complete reaction of Al−Teflon can be described by a two-step global reaction where aluminum particles undergo combustion in the Teflon matrix and then condensation of carbon occurs to form graphite. In the kinetics study of the prototype reaction $Al + SF_6$ by Nelson et al.,[9] rate constants as a function of temperature were measured by monitoring the relative concentrations of either the reactant Al or the primary product AlF using laser-induced fluorescence spectroscopy. From the results, they were able to establish that the reaction proceeds through an atom abstraction transition state under pseudo first-order conditions. In previous work,[5] Dlott and co-workers used time-resolved spectroscopy to look at the Al nanoparticle aggregates termed ALEX in nitrocellulose. Using coherent anti-Stokes Raman scattering to monitor ONO_2 stretching transitions of nitrocellulose, they observed that Al−nitrocellulose chemistry occurred in two stages. In the faster stage, the energy release rate was ∼2 ns. Thus, their ALEX studies provided a preliminary indication of the time dependence of reaction propagation. The spatial dependence problem was nicely addressed by the same authors in a separated publication.[10] Very recently, Zamkov et al.[6] reported a study of the chemical reactions initiated by flash-heating a nanoenergetic material consisting of Al nanoparticle fuel in a Teflon^{AF} oxidizer.

* To whom correspondence should be addressed. E-mail: chaudhuri@wsu.edu. Tel: 509-358 7782. Fax: 509-358 7627.

10.1021/jp810156j CCC: $40.75
Published on Web 04/23/2009

In their study, they used ultrafast mid-infrared spectroscopy to monitor the IR absorption transients of CF_3, CF_2, and COF vibrations. The authors found a faster time constant of $(k_1)^{-1} = 50 \pm 20$ ps for the reaction of Al with COF, and a slower time constant of $(k_2)^{-1} = 0.7 \pm 0.1$ ns for reactions of Al with CF_3 or CF_2. This shows that the reactions with COF are more than 10 times faster than the reactions with CF_3 or CF_2. They finally suggested that reactions of Al with CF_3 and CF_2 have the same apparent rate. Thus, they proposed the possibility of describing the Al + Teflon^{AF} chemistry with just two processes, a slower process involving Al + CF_2 or CF_3 and a faster process involving Al + COF.

Because aluminum burns as a vapor, the first step of this process involves gas-phase reactions between Al and the oxidizers, or between aluminum and the reaction intermediates or reaction products. In this regard, various experimental and theoretical studies have been carried out. Experimentally, the studies range from investigations of the combustion reactions and the intermediate species profiles of hydrofluorocarbons[11] to the kinetics of Al atoms interacting with O_2.[12] As for the theoretical aspect, Catoire[13] and co-worker and Griece at al[14] reported on the thermochemistry of aluminum species for combustion modeling. Detailed theoretical studies of the Al + O_2 reaction have been also reported by Pak et al.[15] and Behler et al.[16] Reactions are also expected to occur on the surface of the aluminum particles as is well documented by the work of Osborne et al.[17] and this heterogeneous chemistry must also be included in a complete model.

In the present study, we report the results of high-level ab initio quantum chemical calculations for the Al species observed, or expected to be present, in the gas phase during Al particle combustion in Teflon. Although the chemistry between Al and Teflon is very complicated, we will only concentrate on the Al−Teflon elementary reactions and will discuss the reaction pathways between aluminum particle and Teflon fragments. We combined the information from the predicted thermochemistry and rate constants to shed light on the mechanism associated with these elementary reactions under both oxygen-rich and oxygen-lean conditions.

2. Computational Methods and Reaction Channels

The ab initio calculations were carried out using the *Gaussian 03* suite of programs.[18] Geometry optimizations and calculation of harmonic vibrational modes for reactants, products, and transition-state structures were performed at the MP2 level[19] using the Pople-type 6-311++G(d,p) and aug-cc-pVDZ basis sets.[20−22] Single-point energies were computed using the coupled-cluster technique with single and double excitations and evaluations by perturbation theory for triple contributions, CCSD(T)[23,24] with the aug-cc-pVTZ[20−22] basis set. We used the Synchronous Transit-Guided Quasi-Newton (STQN) methods,[25,26] for locating transition structures, as implemented in *Gaussian 03*. Intrinsic reaction coordinate (IRC)[27] calculations were carried out to establish the link between transition structures and intermediates. For calculations on species with doublet and triplet spin multiplicity, the value of $\langle S^2 \rangle$ was less than 0.78 and 2.05, respectively. This indicates the good quality of the wave function used for the calculations.[28] We also attempted to carry out density functional theory (DFT) calculations using the popular B3LYP functional, but consistent transition state structures could not be located for some reaction channels, for instance, the CF_2 + Al → CF_2 + AlF channel.

Transition-state theory, introduced by Eyring, Evans, and Polanyi[29,30] in 1935, provided the first theoretical attempt to determine absolute reaction rates. In this theory, a transition state separating reactants and products is used to formulate an expression for the thermal rate constant. A number of assumptions are made in deriving the TST rate expression. The two most basic assumptions are the separation of electronic and nuclear motions, equivalent to the Born−Oppenheimer approximation in quantum mechanics, and that the reactant molecules are distributed among their states in accordance with the Maxwell−Boltzmann distribution. Here, we use the conventional transition-state theory model in which the transition state is located at the saddle point on the potential energy surface and by assuming that a quasi-equilibrium between transition-state species and reactants exists. The rate constants, $k(T)$, for the temperature ranges of 500−900 and 1000−2000 K were calculated with the following expression,

$$k(T) = \Gamma(T)\frac{k_b T}{h}\frac{Q_{TS}}{Q_R}\exp\left(\frac{-E_0}{k_b T}\right) \quad (1)$$

where Q_{TS} and Q_R are the total partition functions for the transition state and reactants or intermediates at temperature T, respectively. E_0 is the energy barrier including zero-point vibrational correction, k_b is Boltzmann's constant, and h is Plank's constant. Here, we adopt the simple Wigner[31] method in the calculation of all possible tunneling corrections for the reactions:

$$\Gamma(T) = 1 + \frac{1}{24}\left(\frac{h\nu}{k_b T}\right)^2 \quad (2)$$

Here, ν is the imaginary frequency at the saddle point.

In this study, we put forth a plausible group of reaction channels for the thermokinetics model of the reaction chemistry in Al−Teflon composites. Accordingly, we explore five different energetic reaction channels between Al and Teflon that might be expressed as

$$CF_3 + Al \rightarrow CF_2 + AlF \quad (I)$$

$$CF_2 + Al \rightarrow CF + AlF \quad (II)$$

$$CF + Al \rightarrow C + AlF \quad (III)$$

$$COF_2 + Al \rightarrow COF + AlF \quad (IV)$$

$$COF + Al \rightarrow CO + AlF \quad (V)$$

Reaction channel III can be decomposed into two subchannels:

$$CF + Al \rightarrow (Al{-}C{-}F)^{IM} \rightarrow C{-}Al{-}F \quad (IIIa)$$

$$C{-}Al{-}F \rightarrow C + Al - F \quad (IIIb)$$

Here channels I, II, and III are for oxygen-deprived conditions. With respect to combustion reactions, the reaction of C_2F_4 with atmospheric oxygen to yield COF_2 and COF has to be considered as well. Channels IV and V describe the scenario for oxygen-rich conditions.

3. Assessment of the Computational Methods

The calculated thermochemistry (enthalpies of reaction) of the Al−Teflon reactions studied in this work, for which experimental data are available, are tabulated in Tables 1 and 2. There is a very good agreement between the calculated values at the MP2/aug-cc-pVDZ level and the corresponding experimental ones in Table 1.

The enthalpies of reaction predicted by the two levels of theory [MP2 and CCSD(T)] in Table 2 are close to each other and are also in good agreement with the experimental values. All of the calculated enthalpies of reaction obtained from the

TABLE 1: Reaction Set for Proposed Combustion Mechanism, Enthalpies of Reaction (in kcal/mol) and Activation Energies (in cal/mol) for the Al−Teflon Chemistry

reaction	$\Delta_r H^a$	$\Delta_r H^b$	rate constant		ref
Thermal decomposition:					
$C_2F_4 \rightarrow CF_2 + CF_2$	68.5	70.2	$8.49 \times 10^{17} \exp(-47085/RT)$	(1)	32
$C_2F_4 \rightarrow CF_3 + CF$	104.8	105.7		(2)	this work
$C_2F_4 + O \rightarrow COF_2 + CF_2$	−94.5	−89.0	$8.13 \times 10^{12} \exp(-1260/RT)$	(3)	32
$F_2 \rightarrow F + F$	36.9	33.0	$2.12 \times 10^{13} \exp(-33723/RT)$	(4)	32
$O_2 \rightarrow O + O$	117.9	117.4	$6.08 \times 10^{15} T^{-1} \exp(-118097/RT)$	(5)	32
Oxidation:					
$CF_3 + O \rightarrow COF_2 + F$	−76.6	−73.4	1.87×10^{13}	(6)	30
$CF_3 + O_2 \rightarrow COF_3 + O$	21.0[c]	25.4	$2.26 \times 10^{9} T^{1.4} \exp(-21402/RT)$	(7)	33
$CF_2 + O \rightarrow COF + F$	−38.0[c]	−38.4	$7.00 \times 10^{13} \exp(-1000/RT)$	(8)	33
$CF_2 + O_2 \rightarrow COF_2 + O$	−45.1	−41.8	$2.01 \times 10^{13} \exp(-26500/RT)$	(9)	28
$CF + O \rightarrow CO + F$	−127.8	−128.0	$4.00 \times 10^{13} \exp(-1000/RT)$	(10)	33
$CF + O_2 \rightarrow COF + O$	−43.0	−42.8	$2.00 \times 10^{13} \exp(-1800/RT)$	(11)	33
$CF + O_2 \rightarrow CO_2 + F$	−135.6	−136.8	9.63×10^{11}	(12)	31
$COF + O \rightarrow CO_2 + F$	−94.0[c]	−93.9	6.00×10^{13}	(13)	32
$COF + O_2 \rightarrow CO_2 + F + O$	25.0[c]	23.6	$2.00 \times 10^{13} \exp(-24000/RT)$	(14)	33
$Al + O_2 \rightarrow AlO + O$	−3.3	16.2	$1.05 \times 10^{14} T^{0.25} \exp(14.5/RT)$	(15)	37
Destruction:					
$CF_3 + F \rightarrow CF_4$	−127.9	−128.4	$1.00 \times 10^{13} \exp(-2000/RT)$	(16)	32
$CF_3 + F_2 \rightarrow CF_4 + F$	−91.0	−94.8	$2.65 \times 10^{12} \exp(-2510/RT)$	(17)	32
$CF_2 + F \rightarrow CF_3$	−86.5	−85.8	7.11×10^{11}	(18)	32
$CF_2 + F_2 \rightarrow CF_3 + F$	−49.5	−52.4	5.01×10^{10}	(19)	32
$CF + F \rightarrow CF_2$	−122.7	−121.3	6.00×10^{13}	(20)	33
$CF + F_2 \rightarrow CF_2 + F$	−85.7	−87.8	2.35×10^{12}	(21)	31
$COF + F \rightarrow COF_2$	−121.0c	−120.3	7.65×10^{12}	(22)	32
$COF + F_2 \rightarrow COF_2 + F$	*N/A*[d]	−86.8	2.71×10^{10}	(23)	32
$COF + COF \rightarrow COF_2 + CO$	*N/A*[d]	−87.9	$2.23 \times 10^{13} \exp(-318/RT)$	(24)	35
$AlF + 2F \rightarrow AlF_3$	−261.6	−258.3		(25)	this work
$AlF + F_2 \rightarrow AlF_3$	−224.6	−224.8		(26)	this work

[a] From CCCBDB Data Base, NIST. Release 14 Sept. 2006, Standard reference Database 101. [b] Calculated at the MP2/aug-cc-pVDZ level of theory. [c] Enthalpy of reaction taken from ref 33. [d] No data given in the NIST Thermochemical Tables.

level of theory used in this study are accurate to within ±1 to ±3 kcal/mol. The most notable exception to this is the enthalpy of reaction for the $Al + O_2 \rightarrow AlO + O$ process, for which the MP2/aug-cc-pVDZ level overestimates it and predicts an opposite sign relative to the experimental value. In general, the enthalpies of reaction predicted by the various levels of theory for the set of reactions in Tables 1 and 2 are in very good agreement with the available experimental values. Without more precise experimental thermochemical and especially gas-phase kinetics data for aluminum reactions with fluorinated compounds, with the exception of SF_6 and NF_3,[9] it is not possible to establish which method performs better for this class of compounds.

3.1. Unrestricted Hartree−Fock Reference. The electronic structure calculations for both local minima and transition states has been carried out based on restricted Hartree−Fock or unrestricted Hartree−Fock wave functions for closed-shell and open-shell systems, respectively. For instance, the triplet state calculations are based on a spin-unrestricted Hartree−Fock (UHF) reference wave function. The spin contamination at the SCF level is very mild for this state ($\langle S^2 \rangle_{UHF} = 2.0137$) and becomes negligible after correlation corrections. It is in fact well-known that electron correlation decreases the spin contamination of the UHF reference states.[32] Thus, based on this discussion we are confident regarding the good quality of the UHF wave function of the triplet states.

3.2. Rigid Rotor Harmonic Approximation. Without accurate spectroscopic data it is almost impossible, at this point, to determine at what temperature the molecular species considered here are excited enough that the rigid rotor-harmonic oscillator approximation begins to become unsatisfactory. As it is well-known, the leading deviations from the RRHO behavior may be attributed to low-frequency torsional motions about single bonds. Two theoretical studies by Truhlar[33] et al. and Lluch[34] et al. have nicely addressed the statistical thermodynamics and the dependence of the rate constants on the treatment of internal rotation modes. In view of their findings and the fact that no pure torsional motions were identified in our transition state structures, the RRHO approximation is fairly good for the temperature ranges considered in this work. Nonetheless, benchmark calculations of accurate partition functions for the molecules considered here are desirable to test the assumptions made in our present study.

4. Results and Discussion

4.1. Combustion Chemistry of C_2F_4 and Aluminum Particles. The combustion mechanism of the Al−Teflon composite requires at first the knowledge of the thermal decomposition of Teflon, polytetrafluoroethylene (PTFE). Decomposition of PTFE begins slowly at 533 K; however, for noticeable decomposition to occur, temperatures above 673 K are needed.[35] Simon and Kaminsky[36] pyrolized PTFE at 773−873 K using steam. According to these authors, the primary decomposition products are tetrafluoroethylene (C_2F_4) and difluorocarbene radicals (CF_2). The constituents of the thermal decomposition reaction in air are mainly carbonyl difluoride, COF_2, C_2F_4, and CF_2, as establish by Baker[35] et al. Carbonyl fluoride was also detected in the combustion process of PTFE.[37] The mass spectrometry analysis of the final product of the thermal degradation of PTFE in tube reactors[38] at temperatures ranging from 583 to 793 K shows an appreciable concentration of several fragments C, CF, CF_2, and CF_3. On the basis of this discussion, we can put forth a plausible group of reaction channels taking place in the combustion process of C_2F_4 as the major Teflon decomposition product. The

TABLE 2: Reaction Enthalpies (in kcal/mol), Entropies of Activation (cal mol^{-1} K^{-1}), Activation Energies (in kcal/mol), and Arrhenius Preexponential Factors (10^{10} s^{-1} and 10^{-10} cm^3 molecule^{-1} s^{-1} for Unimolecular and Bimolecular Reactions, Respectively) Calculated for Five Different Aluminum/Teflon Reaction Channels (Predicted Values for E_a and A Over the Range 1000−2000 K in Parentheses)

		MP2/6-311++G(d,p)				MP2/aug-cc-pVDZ				CCSD(T)/aug-cc-pVTZ[a]			
channel	$\Delta_r H^b$	$\Delta_r H$	$\Delta S^{\ddagger c}$	E_a	A	$\Delta_r H$	$\Delta S^{\ddagger b}$	E_a	A	$\Delta_r H$	E_a	A
Unimolecular:												
I (m = 1)[d]	−73.8	−72.40	0.059	6.02(6.16)	2308.0(2500.0)	−73.10	−0.87	2.82(2.93)	1358.0(1442.5)	−73.17	4.01(4.02)	1359.0(1442.5)
II (m = 2)	−37.6	−37.06	0.29	14.35(14.65)	1230.0(1442.5)	−37.80	−1.88	9.98(10.27)	1070.0(1254.0)	−34.86	12.15(12.90)	1068.0(1247.0)
III	−32.0	−32.55				−35.16				−29.50		
III$_a$ (m = 3)		−63.81	14.83	31.28(31.65)	1037.0(1279.0)	−65.96	17.70	27.00(27.36)	1112.0(1345.0)	−66.59	27.80(28.13)	1112.0(1345.0)
III$_b$ (m = 3)		+ 31.26	3.96	31.52(31.70)	17750.0(19421.8)	+30.80	4.65	31.02(31.20)	10980.0(12018.0)	+37.09	36.71(36.88)	10983.0(12018.0)
IV (m = 2)	*N/A*[e]	−32.94	−5.66	10.30(10.54)	150.5(171.4)	−38.62	−4.92	4.85(5.08)	150.0(171.3)	−35.94	8.52(8.75)	150.2(171.4)
V (m = 1)	*N/A*[e]	−126.90	−2.30	0.67(0.69)	558.0(563.5)	−126.83	−2.19	1.03(1.05)	557.0(563.4)	−123.80	1.85(1.87)	558.0(563.5)
Bimolecular:												
I (m = 3)						−73.10	−20.61	29.27(30.64)	7.60(20.0)	−73.17	31.63(32.98)	7.65(20.0)

[a] Single point calculation at the MP2/aug-cc-pVDZ optimized geometry. [b] From CCCBDB Data Base, NIST. Release 14 Sept. 2006, Standard reference Database 101. [c] $\Delta S^{\ddagger} = S_{tot,TS} - S_{tot,IM}$, where TS and IM are for transition state and intermediate species respectively. $S_{tot} = S_t + S_r + S_v + S_e$. [d] Reaction channel multiplicity. [e] No data given in the NIST Thermochemical Tables.

set of reactions compiled in Table 1 is taken from the chemical kinetic combustion model that has been the subject of both experimental and theoretical investigations over the past four decades. A more detailed analysis of the thermochemical and chemical kinetic data for fluorinated hydrocarbons can be found in the literature[11,39−47] and references therein.

We begin with the scheme in Figure 1 to represent the main reaction paths for a proposed reaction mechanism for the Al−Teflon reaction. The initial C_2F_4 molecules decompose by one of three pathways: thermal dissociation to give CF_2 and CF_3, CF, labeled Decomp-I and Decomp-II respectively, and attack by oxygen atoms. The main intermediates in the mechanism include CF_2, CF_3, CF, COF, and AlF. The resulting stable products are CF_4, COF_2, CO, CO_2, and AlF_3. The chemical steps and rate constants for the combustion of C_2F_4 are tabulated in Table 1. The tabulated values are taken from several experimental and theoretical studies of the C_2F_4 combustion.[11,39−47] Here, we attempted to build a minimal reaction set that could represent the main pathways from reactants to products for a thermokinetic model of the Al−Teflon reactions at both oxygen-rich and -lean conditions.

The oxidation reactions of aluminum atoms are of considerable interest in combustion because aluminum compounds are used as an ingredient in propellant and explosive formulations. Our goal is not to present a systematic study of the reaction of aluminum with oxygen, which has been extensively studied both theoretically[12,48,14,15] and experimentally.[12,49−52] Rather, we focus on the chemistry of reaction 15 in Table 1 and its potential role in the Al−Teflon combustion mechanism. Reaction 15, Al + O_2 → AlO + O, has some interesting features. The reaction products are almost isoenergetic with the reactants, rendering a very low exothermicity of 3.3 kcal/mol compared to the rest of the oxidation reactions in Table 1. A further aspect of this reaction is the possibility of forming AlO_2, Al + O_2 → AlO_2. A theoretical study of the reaction mechanism by Pak and Gordon[15] predicted that the reaction paths leading to AlO + O appear to go through the dissociation of AlO_2, instead of being formed directly from the Al + O_2 reaction. The importance of reaction 15 lies in the belief that it is a major route to the production of atomic oxygen, as it is energetically and most likely kinetically favored over dissociation of molecular oxygen (reaction 5 in Table 1).

Both the frequency factor and the low energy barrier of the Al + O_2 → AlO + O reaction may render this reaction channel very competitive with the combustion of Teflon radicals. A more accurate kinetic model will be required to draw definitive conclusions regarding the relative branching ratios of the AlO, COF, and COF_2 species formed in the earlier steps of the Al−Teflon combustion process.

4.2. Al−Teflon Reaction Channels. The key energetic properties calculated are the enthalpy of reaction in Table 1 and the adiabatic vibrational barrier height, E_0, the entropy of activation $\Delta S^{\ddagger}$, and the enthalpy of reaction ΔH at 298 K in Table 2. The definitions adopted in this work are the following: the adiabatic vibrational barrier height is equal to the difference between the transition state and the intermediate energies added to the difference of the zero-point energies of those species, whereas ΔH is given by the difference of the products' and reactants' energies plus the thermal corrections to the enthalpy. Unless otherwise noted, the results discussed below are those obtained with the highest level ab initio calculations, CCSD(T)/aug-cc-pVTZ//MP2/aug-cc-pVDZ.

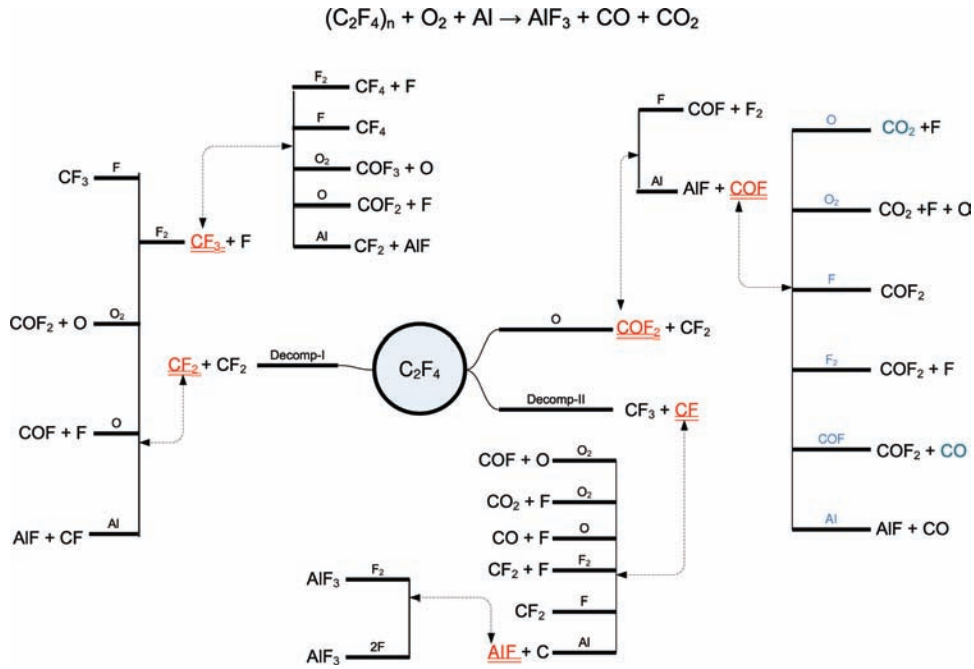

Figure 1. Main reaction paths for the proposed combustion mechanism of the Al−Teflon reactions.

4.2.1. Potential Energy Surfaces of The CF_x + Al, x = 1 − 3 Reactions. A first step toward obtaining a kinetic model is to calculate and characterize both intermediates and transition-state molecular structures for each of the proposed reaction channels. According to the number of electrons of the molecules involved in the reaction channels, we have for their multiplicity the following options: Al−CF_3: 46*e*, $m = 1$ or 3; Al−CF_2: 37*e*, $m = 2$; Al−CF: 28*e*, $m = 1$ or 3; Al−COF_2: 45*e*, $m = 2$; and for Al−COF: 36*e*, $m = 1$ or 3, respectively. Thus, we have explored the following possibilities: (i) for channels I, III, and V, reaction paths following both multiplicity 1 and 3, (ii) for channels II and IV, reaction paths following only multiplicity 2.

The potential energy surfaces of the pathways corresponding to reaction channels I, II, and III predicted from the highest level ab initio calculations, single point CCSD(T)/aug-cc-pVTZ at the optimized MP2/aug-cc-pVDZ geometries, are shown in Figure 2. (a) channel I ($m = 1$), $CF_3 + Al \rightarrow CF_2 + AlF$: The reaction through channel I is exothermic by 73.2 kcal/mol and has a barrier of 3.56 kcal/mol. The structures are displayed in Figure 2. The reaction proceeded through the attack by the aluminum atom to CF_3 carbon and formed a stable intermediate, Al−CF_3 (IM, $m = 1$), as shown in the upper panel of Figure 2. The saddle point can be described as the formation of the new Al−F bond, and the breach of the C−F bond, (TS, $m = 1$). Elimination of the newly formed AlF molecule along with the production of CF_2 radical end this reaction channel. (b) channel I ($m = 3$), $CF_3 + Al \rightarrow CF_2 + AlF$: Unlike the reaction with $m = 1$, there is no intermediate. Thus, the channel proceeds through an atom abstraction transition state (TS, m3), with an activation energy of 30.78 kcal/mol. This energy value is almost 9 times higher than that proceeding with $m = 1$. On the basis of this mechanism, this channel can be described by a bimolecular reaction kinetics. (c) channel II ($m = 2$), $CF_2 + Al \rightarrow CF + AlF$: For this reaction, the predicted barrier is 11.7 kcal/mol, 3.3 times higher than that of the channel I with $m = 1$. The channel is exothermic by 34.8 kcal/mol, which is half of the exothermicity exhibited by I. The reaction starts by the same Al−C interaction and continues to a transition structure, formed by the same forming and breaking process of bonds. It follows the production of AlF and CF radical. (d) channel III ($m = 3$), $CF + Al \rightarrow C + AlF$: Unlike reaction channels I and II, this reaction passes through two transition states until carbon and aluminum fluoride are formed. Russell[53] and co-workers suggested that the complete reaction of Al−Teflon can be described by a two-step global reaction where aluminum particles undergo combustion in the Teflon matrix and then condensation of carbon occurs to form graphite. Although the global enthalpy of reaction is exothermic, −29.5 kcal/mol, its associated barriers are very high (∼30 kcal/mol) compared to those for channels I ($m = 1$) and II. Thus, one might conclude that the formation of graphite needs substantial amounts of energy. It seems to be that the exothermicity of the Al−Teflon reaction is an energy-balance outcome between the energy needed to form carbon and that being released by the AlF formation.

Figure 3 displays the two possible Al−Teflon reaction channels under oxygen-rich conditions. Unlike the mechanism for the oxygen-lean reactions, here the formation of intermediate structures is through the interaction between the aluminum and the oxygen atoms. The corresponding enthalpies of reaction are −35.9 and −123.8 kcal/mol and their barrier heights, 7.89 and 1.61 kcal/mol, respectively. As in the case of reactions under oxygen-lean conditions, the formation of Al−F and breaking of O−Al bonds drive the reaction mechanism. A summary of the predicted thermochemistry is provided in Table 2. From the tabulated values, reaction channel I is the most exothermic followed by channels II and III. In the case of reactions probable under oxygen-rich conditions, channel V is by far the most exothermic. This predicted exothermicity along with the values for the barrier height suggest that channels I and V are expected to react faster under oxygen-deprived and oxygen-rich conditions, respectively. We also attempted to identified reaction paths with $m = 1$ and $m = 3$ for channels III and V respectively but both intermediate and transition states could not be located.

4.2.2. Rate Constants. The results of the ab initio calculations have been used to calculate unimolecular rate constants between 500−900 and 1000−2000 K temperature ranges using eq 1. For each reaction channel, Arrhenius parameters such as

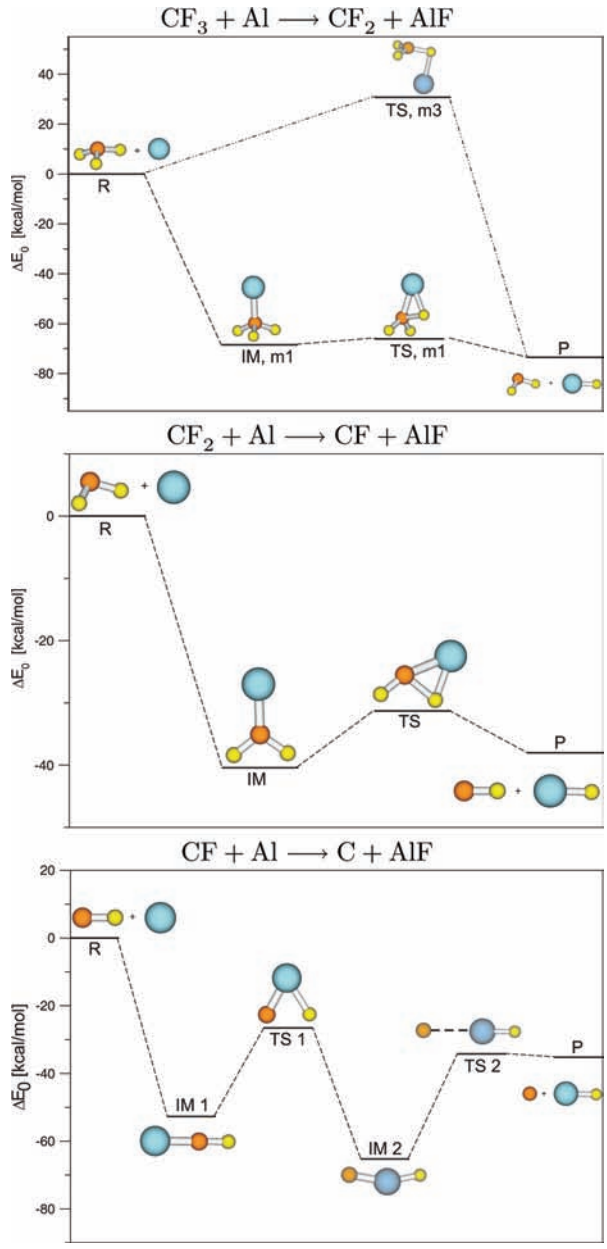

Figure 2. Potential energy surface profile for reaction channels I (upper path for $m = 3$, dashed-dotted trace and lower path for $m = 1$, dashed trace), II, and III calculated at the CCSD(T)/aug-cc-pVTZ//MP2/aug-cc-pVDZ level. In the graphs, IM and TS indicate intermediates and transition state of the respective elementary step.

activation energy, E_a and preexponential factors, A, were extracted. The predicted values of these Arrhenius parameters are tabulated in Table 2. Among the results of Table 2, we also provide the enthalpy of reaction $\Delta_r H$, entropy of activation, $\Delta S^{\ddagger}$, the activation energy E_a, and the preexponential factor A. All five reactions are exothermic with activation energies ranging from 1.85 for channel V to 36.0 kcal/mol for channel III, as predicted by the calculations at the CCSD(T)/aug-cc-pVTZ//MP2/aug-cc-pVDZ level of theory. The predicted preexponential factors for both temperature ranges are reasonable, knowing that the upper limit for unimolecular rate constants at 298 K is roughly 10^{13} s^{-1}. In the bimolecular case, channel I ($m = 3$), the predicted preexponential factor (4.60×10^{14} cm^3 mol^{-1} s^{-1}) for the temperature range 500−900 K, is comparable with the experimentally measured [$(4.10 \pm 1.1) \times 10^{14}$ cm^3 mol^{-1} s^{-1}] for the reaction of aluminum with SF6 as reported by Nelson et al.[9]

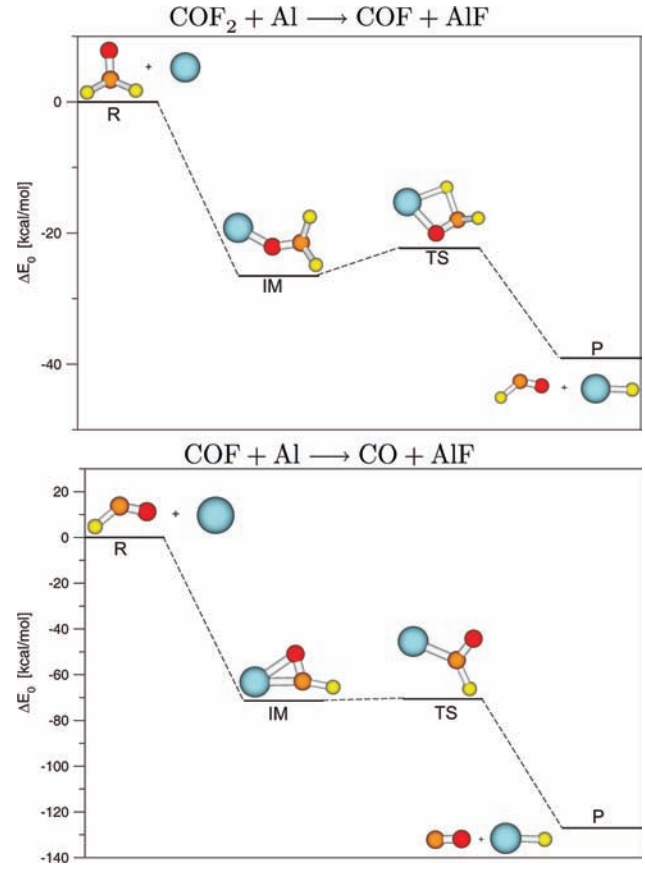

Figure 3. Potential energy surface profile for reaction channels IV and V calculated at the CCSD(T)/aug-cc-pVTZ//MP2/aug-cc-pVDZ level. In the graphs, IM and TS indicate the intermediates and transition state of the respective elementary step.

The rate constants determined from the ab initio calculations are plotted in Arrhenius form in Figure 4. The predicted Arrhenius plots within the 500−900 K temperature range show: (1) On the one hand, reaction channels I with $m = 1$ and V are the fastest among the five proposed reactions. On the other hand, channel I with $m = 3$ is predicted to be unlikely at the temperature ranges of this study, supported by its very negative entropy of activation value of −20.61 cal mol^{-1} K^{-1}. (2) Channels IIIa and IIIb are predicted to be the slowest among the unimolecular reactions. (3) It is interesting to see that the present kinetic model suggests two competitive reaction channels, namely I with $m = 1$ and V. This could be a plausible scenario, as long as both radical species, CF_3 and COF, have significant population under the same thermal conditions. The same can be said for channels II and IV. In the 1000−2000 K range, the kinetic model predicts a tighter scenario for these reaction channels. The branching ratios, that is the ratio of a given channel over the sum of the other channels will give a quantitative picture of the relative efficiencies of the individual reactions as a function of temperature. This is currently a part of our ongoing investigation.

Regression analysis for both temperature ranges yielded the rate constants tabulated in Table 3. For each set of rate constants, Arrhenius parameters were extracted. A summary of the thermokinetic computational results is provided in Table 2.

4.2.3. Comparison with Experiment. Zamkov et al.[6] studied the chemical reactions initiated by flash-heating a nanoenergetic material consisting of Al nanoparticle fuel in a Teflon^{AF} oxidizer. Their experimental findings encouraged us to probe our predicted kinetic model. We first define the quantity τ (ps) to

TABLE 3: Rate Constants (in s^{-1} and $cm^3\ mol^{-1}\ s^{-1}$, for Unimolecular and Bimolecular Reaction, Respectively) from Regression Analysis Using the Calculated Date at the CCSD(T)/aug-pVTZ //MP2/aug-pVDZ Level of Theory (Activation Energies in cal/mol)

reaction	500−900 K	1000−2000 K
Unimolecular:		
I ($m = 1$)	$k(T) = 1.359 \times 10^{13} \exp(-4010/RT)$	$k(T) = 1.442 \times 10^{13} \exp(-4020/RT)$
II ($m = 2$)	$k(T) = 1.068 \times 10^{13} \exp(-12\,150/RT)$	$k(T) = 1.247 \times 10^{13} \exp(-12\,900/RT)$
IIIa ($m = 3$)	$k(T) = 1.112 \times 10^{13} \exp(-27\,800/RT)$	$k(T) = 1.345 \times 10^{13} \exp(-28\,130/RT)$
IIIb ($m = 3$)	$k(T) = 1.0983 \times 10^{14} \exp(-36\,710/RT)$	$k(T) = 1.2018 \times 10^{14} \exp(-36\,880/RT)$
IV ($m = 2$)	$k(T) = 1.50 \times 10^{12} \exp(-8520/RT)$	$k(T) = 1.71 \times 10^{12} \exp(-8750/RT)$
V ($m = 1$)	$k(T) = 5.58 \times 10^{12} \exp(-1850/RT)$	$k(T) = 5.63 \times 10^{12} \exp(-1870/RT)$
Bimolecular:		
I ($m = 3$)	$k(T) = 4.60 \times 10^{14} \exp(-31\,630/RT)$	$k(T) = 1.20 \times 10^{15} \exp(-32\,980/RT)$

be $\tau = 1/k(T)$ in picoseconds. We then used the predicted rate constants for channels I, II, IV, and V to estimate the corresponding τ of each reaction channel. By doing so, we were able to plot τ versus T. The results are displayed in Figure 5 and Figure 6. Figure 5 shows the behavior of τ in the 500−900 K temperature range. As shown in the left panel, the reaction channel V (COF + Al) is faster than the channel I with $m = 1$ (CF_3 + Al). This agrees qualitatively well with the experimental findings of Zamkov et al.[6] From the right panel, one can see that COF_2 + Al reaction is faster than the CF_2 + Al one. Unlike the conclusion drawn in ref 6 that reactions of Al with CF_2 and CF_3 have the same apparent rate, the present kinetic model predicts different rates for CF_3 and CF_2. In fact, the model shows that there is a difference of roughly 3 and 2 orders of magnitude between them for the 500−900 and 1000−2000 K temperature ranges, respectively. Passing to the 1000−2000 K temperature range as shown by Figure 5, now our model interestingly predicts CF_3 + Al with $m = 1$ and CF_2 + Al reaction channels to be faster than COF + Al and COF_2 + Al. Although the calculated rate constants, $k(T)$, for temperatures >1200 K give some insight into the kinetics of the system, clearly they must be used judiciously due to the inherent limitations and the approximations used in this study.

5. Conclusions and Remarks

The rate constants for the gas-phase reactions of the Al−Teflon composite were calculated. The reaction channel I, $m = 1$ (CF_3 + Al) is faster than channels II and III under oxygen-lean conditions, whereas channel V, COF + Al is the faster among the oxygen-rich ones. In addition, the predicted model suggests two competitive reaction channels, namely I and V, as long as they have a significant population under the same thermal conditions. All reaction channels are predicted to be highly exothermic ranging from −29.5 for channel III to −123.8 kcal/mol for channel V, predicted by the most accurate calculations (CCSD(T)/aug-cc-pVTZ//MP2/aug-cc-pVDZ) carried out in this work. The predicted time constants for first-order reactions of

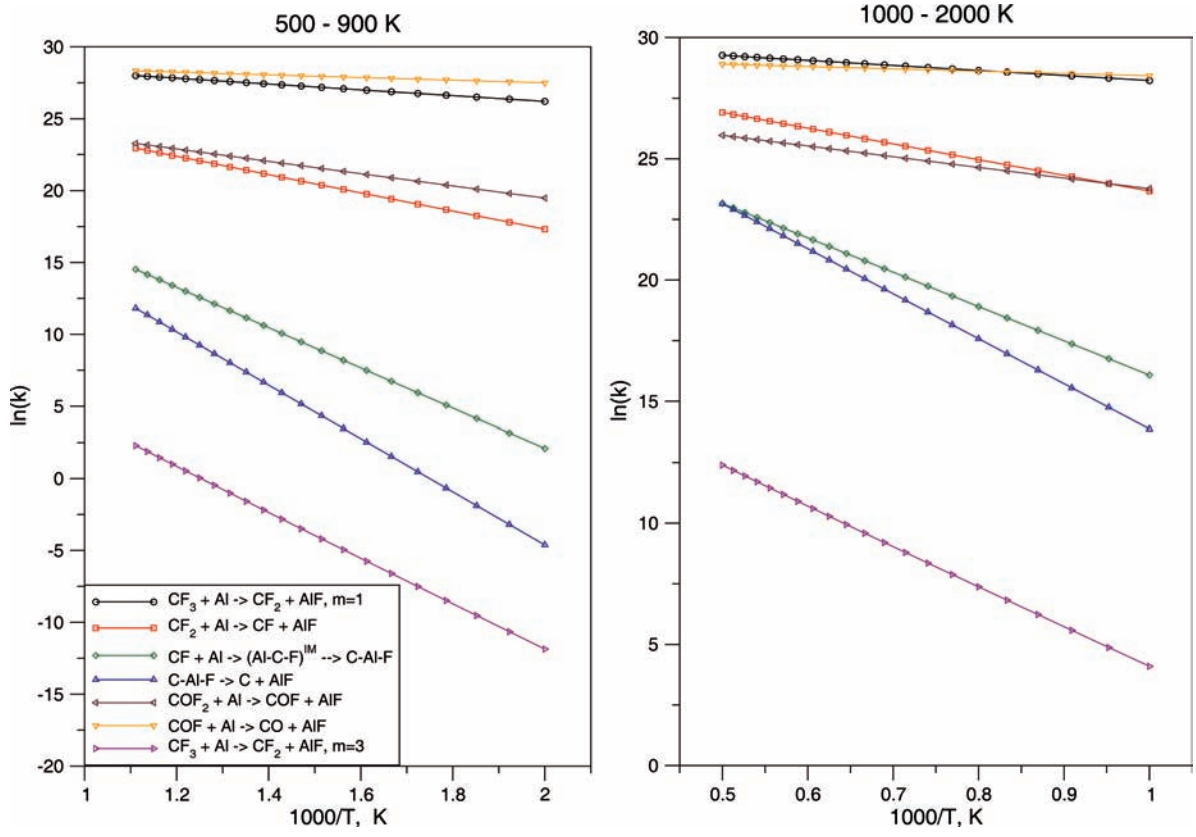

Figure 4. Overall Arrhenius plots for the reaction channels I through V within temperature ranges 500−900 and 1000−2000 K, from the regression analysis at the CCSD(T)/aug-cc-pVTZ//MP2/aug-cc-pVDZ level of theory.

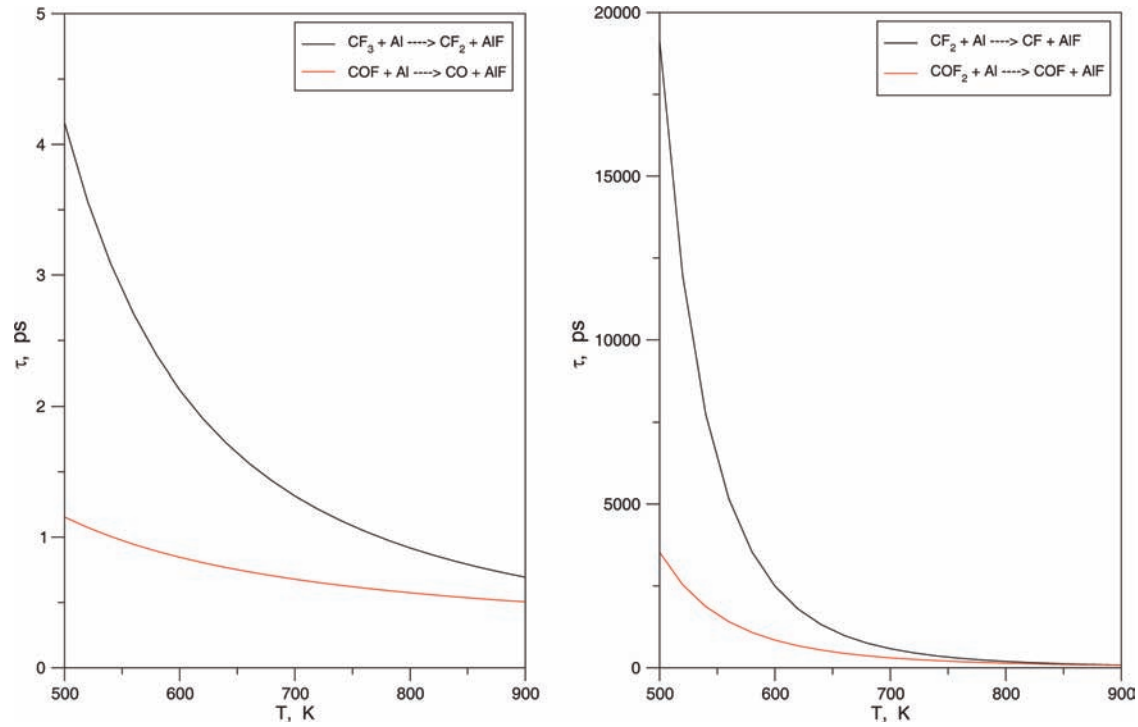

Figure 5. Predicted time constants (τ) for reaction channels I and V (left panel) and reaction channels II and IV (right panel) in the 500−900 K range, calculated at the CCSD(T)/aug-cc-pVTZ//MP2/aug-cc-pVDZ level of theory.

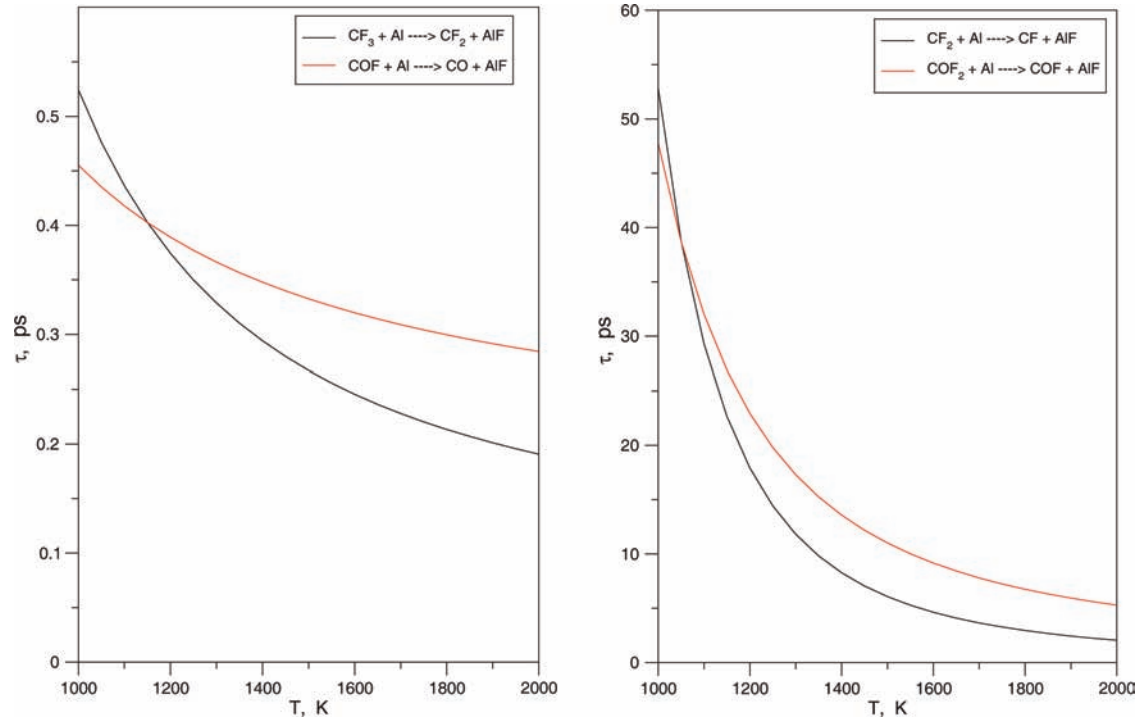

Figure 6. Predicted time constants (τ) for reaction channels I and V (left panel) and reaction channels II and IV (right panel) in the 1000−2000 K range, calculated at the CCSD(T)/aug-cc-pVTZ//MP2/aug-cc-pVDZ level of theory.

Al with CF_3 and COF molecular species are in good agreement with experiment for the 500−1200 K range. On the basis of the present study, the complete reaction of Al−Teflon can be described by a three-step global reaction:

(1) Thermal decomposition of Teflon is facilitated by interactions between alumina surface and fluorine atoms from Teflon. This is an important (not studied in the current work) step toward formation of fluoromethane (CF_3), fluoromethylene (CF_2), carbonyl fluorides (COF_2 and COF) under various concentrations of atmospheric oxygen (combustion) that takes part in subsequent reactions.This combustion process is highly exothermic, −120 kcal/mol (reactions 6−14 in Table 1).

(2) Aluminum particles undergo combustion in both oxygen, reaction 15 and in carbonyl fluorides and fluoromethane−methylene to produce AlO + O and AlF, CO, and CO_2 gases.

The formation of AlF is as exothermic as the previous step, −130 kcal/mol (reactions I−V).

(3) The newly formed AlF molecules will react with fluorine atoms to generate AlF_3, the final product of the aluminum fluorination reactions. This last step is believed to account for the very high exothermicity of the Al−Teflon reaction, as its enthalpy of reaction is predicted to be −258 kcal/mol (reactions 25−26).

Experimental measurements of the enthalpies of reaction and more importantly rates of reaction are required to assent the predictions of the ab initio methods employed in this study. However, the methods used here provide both thermochemical and kinetics parameters of good accuracy to provide preliminary kinetic models of aluminum reacting with fluorinated compounds. These models can be used to identify crucial species, for which additional experimental and theoretical studies can be carried out.

Results from this study will be used to guide the ongoing investigations in our laboratory. Calculations of aluminum surface and alumina clusters are being performed to estimate the importance of size effects and the potential role of the Al_2O_3 oxide layer in the combustion fluorination reactions. Extension of the present TST kinetic model to more accurate methods, such as variational transition state theory,[54] is being pursued (Figure 6).

Acknowledgment. The authors want to thank Dr. Y. M. Gupta for suggesting this problem and for subsequent discussions. Dr. C. S. Yoo is thanked for many discussions. This work was supported by the Office of Naval Research under Grant No. N00014-06-1-0315.

Supporting Information Available: Cartesian coordinates, harmonic vibrational frequencies, and infrared intensities for reactants, products, and transition state structures calculated at the MP2/aug-cc-pVDZ level of theory. This material is available free of charge via the Internet at http://pubs.acs.org.

References and Notes

(1) Dlott, D. D. *Annu. Rev. Phys. Chem.* **1999**, *50*, 251.
(2) Miziolek, A. W. *AMPTIAC* **2002**, *5*, 43.
(3) Granier, J. J.; Pantoya, M. L. *Combust. Flame* **2004**, *138*, 373.
(4) Plantier, K. B.; Pantoya, M. L.; Gash, A. E. *Combust. Flame* **2005**, *140*, 299.
(5) Yang, Y.; Sun, Z.; Wang, S.; Dlott, D. D. *J. Phys. Chem. B* **2003**, *107*, 4485.
(6) Zamkov, M. A.; Conner, R. W.; Dlott, D. D. *J. Phys. Chem. C* **2007**, *111*, 10278.
(7) Dlott, D. D. *Mater. Sci. Technol.* **2006**, *22*, 463.
(8) Parker, J. K.; Garland, N. L.; Nelson, H. H. *J. Phys. Chem. A* **2002**, *106*, 307.
(9) Parker, L. J.; Ladouceur, H. D.; Russell, T. P. *AIP Conf. Proc.* **2000**, *505*, 941.
(10) Yang, Y.; Shufeng, W.; Sun, Z.; Dlott, D. D. *J. Appl. Phys.* **2004**, *95*, 3667.
(11) L'espérance, D.; Wlliams, B. A.; Fleming, J. W. *Combust. Flame* **1999**, *117*, 709.
(12) Le Picard, S. D.; Canosa, A.; Travers, D.; Chastaing, D.; Rowe, B. R.; Stoecklin, T. *J. Phys. Chem. A* **1997**, *101*, 9988.
(13) Swihart, M. T.; Catoire, L. *Combust. Flame* **2000**, *121*, 210.
(14) Politzer, P.; Lane, P.; Grice, M. E. *J. Phys. Chem. A* **2001**, *105*, 7473.
(15) Pak, M. V.; Gordan, M. S. *J. Chem. Phys.* **2003**, *118*, 4471.
(16) Behler, J.; Delley, B.; Lorenz, S.; Reuter, K.; Scheffeler, M. *Phys. Rev. Lett.* **2005**, *94*, 036104.
(17) Osborne, D. T.; Pantoya, M. L. *Combust. Sci. Technol.* **2007**, *179*, 1467.
(18) Frisch, M. J. ; Trucks, G. W.; Schlegel, H. B.; Scuseria, G. E.; Robb, M. A.; Cheeseman, J. R.; Montgomery, J. A., Jr.; Vreven, T.; Kudin, K. N.; Burant, J. C.; Millam, M.; Iyengar, S. S.; Tomasi, J.; Barone, V.; Mennucci, V.; Cossi, M.; Scalmani, G.; Rega, N.; Petersson, G. A.; Nakatsuji, H.; Hada, M.; Ehara, M.; Toyota, K.; Fukuda, R.; Hasegawa, J.; Ishida, M.; Nakajima, T.; Honda, Y.; Kitao, O.; Nakai, H.; Klene, M.; Li, X.; Knox, J. E.; Hratchian, H. P.; Cross, J. B.; Adamo, C.; Jaramillo, J.; Gomperts, R.; Stratmann, R. E.; Yazyev, O.; Austin, A. J.; Cammi, R.; Pomelli, C.; Ochterski, J. W.; Ayala, P. Y.; Morokuma, K.; Voth, G. A.; Salvador, P.; Dannenberg, J. J.; Zakrzewski, V. G.; Dapprich, S.; Daniels, A. D.; Strain, M. C.; Farkas, O.; Malick, D. K.; Rabuck. A. D.; Raghavachari, K.; Foresman, J. B.; Ortiz, J. V.; Cui, Q.; Baboul, A. G.; Clifford, S.; Cioslowski, J.; Stefanov, B. B.; Liu, G.; Liashenko, A.; Piskorz, P.; Komaromi, I; Martin, R. L.; Fox, D. J.; Keith, T.; Al-Laham, M. A.; Peng, C. Y.; Nanayakkara, A.; Challacombe, M.; Gill, P. M. W.; Johnson, B.; Chen, W.; Wong, M. W.; Gonzalez, C.; Pople, J. A. *Gaussian 03*, Revision B.05; Gaussian, Inc.: Pittsburgh, PA, 2003.
(19) Møller, C.; Plesset, M. S. *Phys. Rev.* **1934**, *46*, 618.
(20) Dunning, T. H., Jr. *J. Chem. Phys.* **1989**, *90*, 1007.
(21) Kendall, R. A.; Harrison, R. J.; Dunning, T. H., Jr. *J. Chem. Phys.* **1992**, *96*, 6796.
(22) Woon, D. E.; Dunning, T. H., Jr. *J. Chem. Phys.* **1993**, *98*, 1358.
(23) Purvis, G. D., III.; Bartlett, R. J. *J. Chem. Phys.* **1982**, *76*, 1910.
(24) Raghavachari, K.; Trucks, G. W.; Pople, J. A.; Head-Gordon, M. *Chem. Phys. Lett.* **1989**, *157*, 479.
(25) Peng, C.; Ayala, P. Y.; Schlegel, H. B.; Frish, M. J. *J. Comput. Chem.* **1996**, *17*, 49.
(26) Peng, C.; Schlegel, H. B. *Israel J. Chem.* **1994**, *33*, 449.
(27) Gonzales, C.; Schlegel, H. B. *J. Phys. Chem.* **1990**, *94*, 5523.
(28) Szabo, A.; Ostlund, N. S. *Modern Quantum Chemistry*, Dover Publications: Mineola, NY, 1989.
(29) Eyring, H. *J. Chem. Phys.* **1935**, *3*, 107.
(30) Evans, M. G.; Polanyi, M. *Trans. Faraday Soc.* **1935**, *31*, 875.
(31) Wigner, E. P. *J. Chem. Phys.* **1937**, *5*, 720.
(32) Sekino, H.; Barlett, R. J. *J. Chem. Phys.* **1985**, *82*, 4225.
(33) Chuang, Y.-Y.; Truhlar, D. G. *J. Chem. Phys.* **2000**, *112*, 1221.
(34) Masgrau, L.; Gonzalez-Lafont, A.; Lluch, J. *J. Comput. Chem.* **2003**, *24*, 701.
(35) Baker, B. B.; Kasprzak, D. J. *Polym. Degrad. Stab.* **1993**, *42*, 181.
(36) Simon, C. M.; Kaminsky, W. *Polym. Degrad. Stab.* **1998**, *62*, 1.
(37) Conesa, J. A.; Font, R. *Polym. Eng. Sci.* **2001**, *41*, 2137.
(38) McKinnon, J. T.; Duan, H. M. NASA Report *N96−15574*, 147.
(39) Modica, A. P.; Sillers, S. J. *J. Chem. Phys.* **1968**, *48*, 3283.
(40) Keating, E. L.; Matula, R. A. *J. Chem. Phys.* **1977**, *66*, 1237.
(41) Ryan, K. R.; Plumb, I. C. *J. Phys. Chem.* **1982**, *86*, 4678.
(42) Tsai, C.; Belanger, S. M.; Kim, J. T.; Lord, J. R.; McFadden, D. L. *J. Phys. Chem.* **1989**, *93*, 1916.
(43) Peeters, J.; van Hoeymissen, J.; Vanhaelemeersch, S.; Vermeylen, D. *J. Phys. Chem.* **1992**, *96*, 1257.
(44) Douglass, C. H.; Ladouceur, H. D.; Shamamian, V. A.; McDonald, J. R. *Combust. Flame* **1995**, *100*, 529.
(45) Burgess, D. R., Jr.; Zachariah, M. R.; Tsang, W.; Westmoreland, P. R. *Prog. Energy Combust. Sci.* **1996**, *21*, 453.
(46) Asher, R. L.; Appelman, E. H.; Ruscic, B. *J. Chem. Phys.* **1996**, *105*, 9781.
(47) Yamamori, Y.; Takahashi, K.; Inomata, T. *J. Phys. Chem. A* **1999**, *103*, 8803.
(48) Reignier, D.; Stoecklin, T.; Le Picard, S. D.; Canosa, A.; Rowe, B. R. *J. Chem. Soc., Faraday Trans.* **1998**, *94*, 1681.
(49) Naulin, C.; Costes, M. *Chem. Phys. Lett.* **1999**, *310*, 231.
(50) Pangilian, G. I.; Russell, T. P. *J. Chem. Phys.* **1999**, *111*, 445.
(51) Honma, K. *J. Chem. Phys.* **2003**, *119*, 3641.
(52) Ishida, M.; Higashiyama, T.; Matsumoto, Y.; Honma, K. *J. Chem. Phys.* **2005**, *122*, 204312.
(53) Parker, L. J.; Ladouceur, H. D.; Russell, T. P. *AIP Conference Proceedings* **2000**, *505*, 941.
(54) Truhlar, D. G.; Garrett, B. C.; Klippenstein, S. J. *J. Phys. Chem.* **1996**, *100*, 12771.

JP810156J